Available online at www.sciencedirect.com
ScienceDirect
Continental Shelf Research 26 (2006) 1971–1983
CONTINENTAL SHELF RESEARCH
www.elsevier.com/locate/csr

Assessment of groundwater discharges into West Neck Bay, New York, via natural tracers

H. Dulaiova[a,1], W.C. Burnett[a,*], J.P. Chanton[a], W.S. Moore[b], H.J. Bokuniewicz[c], M.A. Charette[d], E. Sholkovitz[d]

[a]*Department of Oceanography, Florida State University, Tallahassee, FL 32306, USA*
[b]*Department of Geological Sciences, University of South Carolina, Columbia, SC 29208, USA*
[c]*Marine Sciences Research Center, State University of New York, Stony Brook, NY 11794, USA*
[d]*Department of Marine Chemistry and Geochemistry, Woods Hole Oceanographic Institution, Woods Hole, MA 02543, USA*

Received 8 December 2004; received in revised form 22 May 2006; accepted 19 July 2006
Available online 1 September 2006

Abstract

A field experiment to compare methods of assessing submarine groundwater discharge (SGD) was held on Shelter Island, NY, in May 2002. We evaluated the use of radon, radium isotopes, and methane to assess SGD rates and dynamics from a glacial aquifer in the coastal zone. Fluxes of radon across the sediment-water interface were calculated from changes in measured surface water inventories following evaluation and correction for tidal effects, atmospheric evasion, and mixing with offshore waters. These fluxes were then converted to SGD rates using the measured radon concentration in the groundwater. We used the short-lived radium isotopes to calculate a horizontal mixing coefficient to assess radon loss by mixing between nearshore and offshore waters. We also made an independent calculation of SGD using the Ra-derived mixing coefficient and the long-lived ^{226}Ra concentration gradient in the bay. Seepage rates were calculated to range between 0 and 34 cm day^{-1} using the radon measurements and 15 cm day^{-1} as indicated by the radium isotopes. The radiotracer results were consistent and comparable to SGD rates measured directly with vented benthic chambers (seepage meters) deployed during this experiment. These meters indicated rates between 2 and 200 cm day^{-1} depending on their location. Both the calculated radon fluxes and rates measured directly by the automated seepage meters revealed a clear reproducible pattern of higher fluxes during low tides. Considering that the two techniques are completely independent, the agreement in the SGD dynamics is significant. Methane concentration in groundwater was very low (~30 nM) and not suitable as SGD tracer at this study site.

Keywords: Submarine groundwater discharge; Radiotracers; Radon; Radium; Methane; Shelter Island NY

1. Introduction

It is now recognized that in certain regions the direct discharge of groundwater into the coastal oceans can be significant. Whether in form of fresh groundwater or recirculated seawater, submarine groundwater discharge (SGD) complements river

*Corresponding author. Tel.: +1 850 644 6703; fax: +1 850 644 2581.
E-mail address: wburnett@mailer.fsu.edu (W.C. Burnett).
[1]Present address: Department of Marine Chemistry and Geochemistry, Woods Hole Oceanographic Institution, Woods Hole, MA 02543, USA.

0278-4343/$ - see front matter © 2006 Elsevier Ltd. All rights reserved.
doi:10.1016/j.csr.2006.07.011

inputs, as a quantitatively smaller, but still important source of solutes into the coastal zone. SGD is, therefore, of both hydrological and oceanographical concern because of its influence on the water balance on land and biogeochemical inputs into the ocean (Johannes, 1980; D'Elia et al., 1981; Valiela et al., 1990; Laroche et al., 1997; Boehm et al., 2004). Still, assessments of groundwater discharge rates and associated chemical mass flux remain difficult due to a high degree of uncertainty in the methodologies. There is also a strong temporal variation in these fluxes due to tides and the difference in hydraulic gradients between wet and dry seasons (Michael et al., 2005), and spatial variations due to different geographical settings and anisotropy of coastal sediments (Moore, 1999; Burnett et al., 2001a; Taniguchi et al., 2002).

The basic approaches for quantitative assessments of groundwater discharge include hydrologic modeling, direct physical measurement using seepage meters, and tracer techniques. A series of systematic comparisons of assessment methods has been performed over the past few years under sponsorship by the Scientific Committee on Oceanic Research (SCOR), the Land-Ocean Interactions in the Coastal Zone (LOICZ) project, UNESCO's Intergovernmental Oceanographic Commission (IOC) and International Hydrologic Project (IHP), and the International Atomic Energy Agency (IAEA). These systematic comparisons are conducted at a series of sites selected as coastal "prototypes" representative of important types of coastline selected by the LOICZ typology group (Bokuniewicz, 2001). In addition to comparing differing approaches of tracers for the evaluation of SGD, an additional goal of the project is to determine which tracers/approaches are best applicable in certain coastal situations or at certain types of coastlines to offer guidance to future researchers. We report here on the geochemical tracer results of one of these experiments held on Shelter Island, New York, May 17–22, 2002. This site represents a glacial till setting. The techniques applied by various investigators included manual, heat-based, ultrasonic, and dye-dilution-based automated seepage meters deployed side-by-side at the study site; geoelectric measurements of the area; and the use of naturally occurring geochemical tracers. Estimates of groundwater discharge in the area had previously been made by water balance calculations and hydrogeologic modeling (DiLorenzo and Ram, 1991; Schubert, 1998).

Geochemical tracers have been used successfully for assessment of SGD in a number of other studies. For example, Moore used radium isotopes as a tracer in a series of papers reporting on the quantity and effects of SGD off the coast of the southeastern US (Moore, 1996; Moore, 2000a, b). Others used radium isotopes to study SGD and coastal residence times (Krest and Harvey, 2003; Charette et al., 2001; Kelly and Moran, 2002; Kim et al., 2005). Radon has also been shown to be an excellent tracer for work performed in the Gulf of Mexico (Cable et al., 1996a; Burnett et al., 2002; Burnett and Dulaiova, 2003), in Florida Bay (Chanton et al., 2003; Corbett et al., 1999, 2000) and Eckernforde Bay (Sauter et al., 2001). Radon and radium isotopes are radioactive elements from the uranium and thorium natural decay series, which are relatively easy to measure, and (except for atmospheric exchange in the case of radon) they behave conservatively in coastal ocean waters.

Methane has been employed as a tracer of groundwater inputs into near-shore waters along the coast of the northeastern Gulf of Mexico (Bugna et al., 1996 and Cable et al., 1996b), Florida Bay (Corbett et al., 1999), Eckernforde Bay (Schluter et al., 2004), and Korea (Kim and Hwang, 2002). Although methane is not a conservative tracer it has proven to be useful where its concentration in groundwater highly exceeds methane inventories in the water column.

One of the advantages of geochemical tracers over seepage meters is that the coastal water column integrates the tracers and smoothes small-scale spatial variations in discharge. In this study, we show that while radium isotopes as well as radon have been shown to be effective tracers of SGD, they are even more powerful when applied together in the same system. This paper will illustrate the strength of estimating SGD from the combination of radon and radium tracers.

2. Study site and methods

West Neck Bay (WNB) is a shallow, enclosed embayment located on Shelter Island in the eastern half of the Peconic Bay, New York. The unconfined surface aquifer on Shelter Island is composed of unconsolidated fine-to-medium coarse sands and is called the upper glacial aquifer. It is recharged solely by precipitation. The aquifer has high hydraulic heterogeneity; the hydraulic conductivity as well as the hydraulic gradient varies along the

coastline of the island. The upper glacial aquifer is underlain by base clay at ~27 m below sea level. Groundwater in the deeper (100 m) aquifer on the island is mostly saline (Schubert, 1998). The subject of our study was groundwater discharging from the surface aquifer and our study site was located in the northeastern part of WNB (Fig. 1). The bottom sediment in the bay is mostly sand with muddy deposits. Paulsen et al. (2001) measured high SGD rates ranging between 60 and 240 cm day^{-1} occurring along this section of the shoreline using an ultrasonic flow meter connected to a steel collection funnel. Their measurements also showed that most of groundwater discharge occurs at about a 50-m wide section of the shore.

During the intercomparison experiment, we collected water samples in the WNB vicinity (Fig. 1) and analyzed them for radon, radium isotopes, and methane. For the radium isotope analysis, water samples of large volume (20–100 L) were collected from wells and piezometers using a peristaltic pump, ambient seawater samples were collected at ~1 m depth or at mid-depth using a high-flow diaphragm pump, and collected from seepage meters using a peristaltic pump drawing water at a very slow rate (0.1–0.2 L min^{-1}) or using bags attached to the vented chambers. We measured the salinity of each sample and than passed the water through MnO_2-coated acrylic fiber that retains radium, thorium, and actinium (Moore, 1976). The fibers were counted for ^{223}Ra, ^{224}Ra, and ^{228}Th on a delayed coincidence counter system (Moore and Arnold, 1996). ^{226}Ra and ^{228}Ra were measured by leaching and barium sulfate co-precipitation followed by gamma-spectrometry at the University of South Carolina (Moore, 2000a). Smaller volume samples (0.25–5 L) were collected using a peristaltic pump for ^{222}Rn measurements. Radon activities in grab samples were determined using a radon-in-air monitor (RAD-7, Durridge Co., Inc.) with an adaptor for water samples (RAD-H_2O) and by a standard radon emanation technique with a newly-designed plastic bottle (Stringer and Burnett, 2004). Methane samples in groundwaters were collected into 50-mL glass bottles and analyzed by headspace equilibration technique and flame ionization gas chromatography. Methane analyses of coastal seawater at the site were collected in a semi-continuous manner by equilibration in an air-water exchanger as described later in this paper.

Six sediment samples were collected from several places in the seepage-meter measurement area to assess radon pore water concentrations by a sediment equilibration technique (Corbett et al., 1998). Sediment samples of approximately 150-g wet weight were equilibrated with 300 mL of deionized water in stoppered Erlenmayer flasks. The stoppers had two tubes attached to them that served as inlet and outlet for helium carrier gas during analysis. For a period of at least 21 days

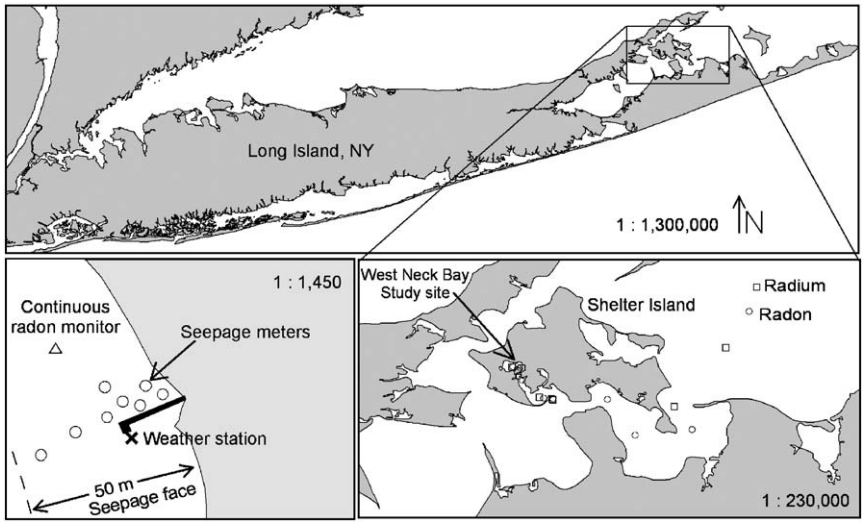

Fig. 1. Map of Long Island, New York, with an inlay of Shelter Island and the geochemical tracer sampling stations. The squares indicate the radium and circles represent the radon sampling points. Also included is a detailed sketch of the study site in West Neck Bay indicating the locations of the continuous radon monitor, weather station, and seepage meters.

(~5.5 half-lives of ^{222}Rn) these tubes were clamped and the flasks were agitated on a shaker table to allow the radon to escape from the sediment into the fluid phase. After this period the accumulated ^{222}Rn in the fluid was measured by the emanation technique.

Water samples for radium, radon, and methane were also collected on an approximately 20-km long transect leading from the study site at WNB to the south and then east to open waters in Gardiners Bay (Fig. 1). These samples were collected from the top 1-m of the water column using a submersible pump.

In order to assess temporal variations in groundwater seepage rates, we also made continuous methane and radon measurements in the water column at the WNB study site. We deployed a continuous radon monitor (Burnett et al., 2001b) on a boat anchored ~25 m from the shoreline where the water depth ranged from 0.7–1.4 m (Fig. 1). This system consists of a submersible pump attached to the boat and reaching to a depth of about 0.7 m below surface. The water depth and therefore the pump distance from the bottom changed due to the tides but the pump's fixed depth from the water surface ensured a constant hydraulic head and steady water flow rate. This way the pump was bringing a steady stream of water to an air–water exchanger where radon is degassed and delivered to a commercial radon-in-air analyzer. The instrument made integrated measurements of radon concentration in the seawater every 2 h over a 7-day period. On a nearby dock we installed a water level meter (to monitor the tides), a radon-in-air monitor, and weather station, which made continuous measurements of wind speed, air and water temperature.

On the same boat as the continuous radon monitor we also measured methane using an equilibration sampler similar to that of radon. Bay water was pumped into a 3-L chamber and sprayed into the headspace at a rate of 1–1.5 L min^{-1}. The headspace (about 1 L) was flushed with nitrogen at a rate of 20 mL min^{-1}. The air from the headspace was vented via a one-way valve. Since we did not have a continuous methane analyzer, headspace methane samples were taken every 15 min during selected periods of the experiment using a syringe and were analyzed by flame ionization gas chromatography.

3. Results

A summary of results from water samples analyzed for radium isotopes, Rn, methane, and salinity is shown in Table 1. Radium isotope activities were lower in wells and piezometers where the salinity of the samples was 0‰. This was expected because radium isotopes in freshwater environments are predominantly bound to particles. The radium concentrations increased markedly in water collected from the seepage meters, because groundwater carries radium released from aquifer solids to the coastal waters. The radium concentration in these samples also depended on the time of sample collection because SGD at this site tends to be the highest at low tide and higher groundwater discharge brings more radium into the chambers. The ranges of the measured activities are displayed in Table 1, where the higher values are from samples collected at low tides and the lower values correspond to samples collected at high tides. The variation of radium isotope activities in surface waters as a function of distance offshore on the 20-km long transect leading from the WNB study site shows that all radium isotopes have high activities near the coast and decreasing activity with increasing distance (Fig. 2). Seawater samples collected

Table 1
Ranges of activities (dpm m^{-3}) of excess ^{222}Rn, ^{223}Ra, excess ^{224}Ra, ^{226}Ra, ^{228}Ra, methane (nM), and salinity (ppt) measured in wells, piezometers (have narrower screen than wells), seepage meters and seawater within 50 meters from the shore from the West Neck Bay study site

	Ex. ^{222}Rn (dpm m^{-3})	^{223}Ra (dpm m^{-3})	Ex. ^{224}Ra (dpm m^{-3})	^{226}Ra (dpm m^{-3})	^{228}Ra (dpm m^{-3})	Methane (nM)	Salinity (ppt)
Wells	150,000–360,000 (15)	<10 (2)	40–80 (2)	60–340 (4)	120–200 (2)	4–30 (7)	0–0.1
Piezometers	150,000–250,000 (8)	<10 (2)	50–70 (2)	70–150 (2)	280 (2)	14–35 (6)	0–0.1
Seepage meters	3000–30,000 (9)	10–240 (9)	200–2800 (9)	60–370 (12)	270–1700 (9)	8–33 (2)	25.3–28.2
Seawater	1000–12,000 (82)	40–60 (11)	220–440 (11)	130–180 (23)	600–900 (11)	11–37 (170)	26.2–29.3

"Ex." refers to excess activities unsupported by radioactive parents. The numbers in parenthesis indicate the number of samples analyzed.

from the seepage meters (Table 1) and within 50 m from the shore were distinctly enriched in radium isotopes compared to offshore samples. The near-shore waters are highest in the thorium-series nuclides ^{228}Ra and ^{224}Ra with the uranium-series isotopes ^{226}Ra and ^{223}Ra being much lower. This is likely a reflection of the predominance of Th over U in the aquifer sediments and the different regeneration times of radium isotopes from their Th parents.

Radon activity (Table 1) was highest in wells and piezometers where the water was in contact with material containing its parent ^{226}Ra. ^{226}Ra is mainly attached to particles and decays to ^{222}Rn that tends to escape because of alpha recoil processes and its gaseous state into the surrounding water. Radon activities in wells and piezometers were up to two orders of magnitude higher than in the coastal seawater. On the transect leading from the study site offshore, radon activities were highest near the coast and showed a decreasing pattern with distance similar to the ^{224}Ra pattern. Results of radon activities in wells and from the sediment equilibration experiments are shown in Table 2.

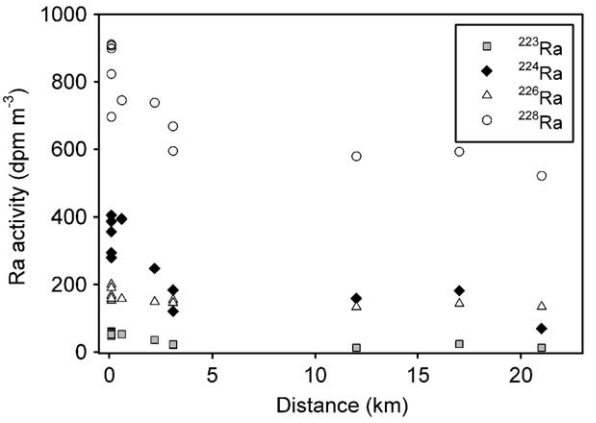

Fig. 2. Activities of radium isotopes (dpm m^{-3}) for samples collected in the West Neck Bay study site and on the transect leading from the study site to Gardiners Bay.

Methane concentrations within groundwater were not always enriched over bay water concentrations thus ruling out the use of methane as an SGD tracer in this environment. This may have been a result of its non-conservative nature, and its production in the water column or low production in the aquifer.

The continuous ^{222}Rn and methane records together with the observed water levels are shown in Fig. 3. The methane record is not continuous throughout the entire study period because it required manual sampling (the radon is completely automated). The continuous radon record clearly changes with a 12-h periodicity, apparently due to the increase in hydraulic gradient at low tides causing increased seepage and higher radon fluxes. That is why the highest increase (largest positive slope in the radon concentrations in Fig. 3) occurs when the tides are the lowest. The radon activities increase continuously almost until the tide changes to flood tide when the activities start to decrease due

Table 2
Activities of ^{222}Rn measured in wells adjacent to the study site and pore water estimates based on sediment equilibration techniques

Sample	Location	Sediment Porosity	Bulk density (g cm^{-3})	^{222}Rn (dpm m^{-3})	S.D.
Beach seep	Beach at low tide			164,000	32,000
Piezometer	10′			192,000	28,000*
Well S-1	S-1 B			363,000	65,000*
	S-1 C			367,000	64,000
	S-1 D			348,000	18,000*
Well S-2				158,000	23,000*
Tap water	Pridwin Hotel			201,000	52,000*
	Piezometers	0.26	1.74	183,000	30,000*
Sediment equilibration experiment	Stony Brook 2	0.37	2.05	154,000	21,000*
	FSU 1	0.41	1.93	177,000	54,000*
	K 2	0.45	2.02	166,000	18,000
	K 1	0.52	1.66	151,000	14,000
	Small Krupaseep	0.45	1.78	179,000	17,000
Average (excluding S-1)				173,000	17,000

Standard deviations with asterisks indicate duplicates, otherwise S.D. estimated via counting statistics. Radon values from well cluster S-1, thought to be influenced by heterogeneity in the aquifer, were excluded from the average.

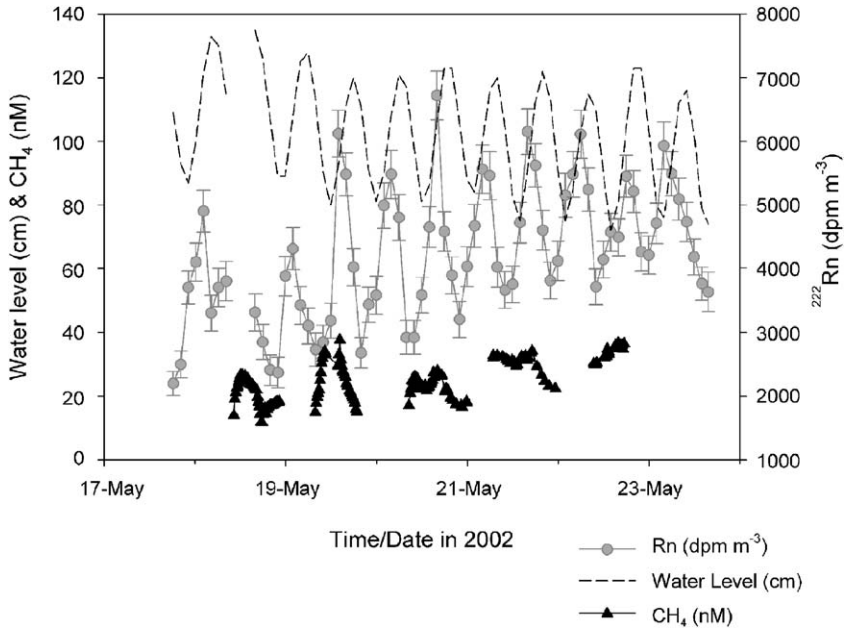

Fig. 3. Continuous ^{222}Rn measurements (dpm m^{-3}), methane (CH_4), and water level (tidal range 0.6 m) records from the study site in West Neck Bay. Radon and methane concentrations tend to be the highest shortly after the lowest tide.

to lower seepage therefore lower radon flux and mixing with low concentration offshore waters.

4. Discussion

4.1. Calculation of SGD using radium isotopes

The results from radium isotopes and radon analyses indicate that all these tracers have potential to be good SGD tracers, and their combination allows us to evaluate the magnitude and dynamics of local and regional groundwater flow at the same time. The spatial distribution of radium isotopes on the transect leading from the WNB study site going offshore to Gardiners Bay (Fig. 2) allows us to quantify material flux from the coastal area to offshore. All four radium isotope activities display an apparent break in slope at a distance of about 4 km from the beginning of the transect. This distance corresponds to the mouth of the WNB inlet. There were no samples collected between ~4–12 km from the study site. Samples beyond 12 km were collected in Shelter Island Sound and Gardiners Bay. The break in slope could thus be a result of different mixing patterns in the sound than WNB. Since we are interested mainly in the processes in the nearshore area, we will restrict the use of these results to the first 4 km in WNB.

A previous study of West Neck Sound reported a water residence time of about 11.7 days (DiLorenzo and Ram, 1991). On this time scale, the radioactive decay of ^{226}Ra (half-life: 1600 yr) and ^{228}Ra (5.7 yr) can be neglected. From our results it appears that both long-lived radium isotopes have a linear trend with distance on the 4-km long part of the transect that may indicate that their distribution is controlled more by diffusive mixing than advection. Advection would cause negative or positive curvature of the activity of the long-lived radium isotopes depending on its direction offshore or onshore. In systems controlled by eddy diffusion an eddy diffusion coefficient (K_h) can be calculated applying a principle developed by Moore (2000a) using the distributions of short-lived ^{223}Ra (half-life: 11.4 d) or ^{224}Ra (3.6 d). The patterns of these short-lived radium isotopes with distance offshore will depend on two processes, radioactive decay and mixing. The decay rates are known and the mixing rates can thus be estimated based on the slope of the natural logarithm of activity as a function of distance. The distributions of both short-lived isotopes reflect mixing on a several-day long time scale. Because of its longer half-life the ^{223}Ra profile is preferable since short-term disturbances would be smoothed out (Fig. 2). The plot of ln ^{223}Ra versus distance (Fig. 4a) has a slope of $-0.289 \pm 0.029\,\mathrm{km}^{-1}$ from

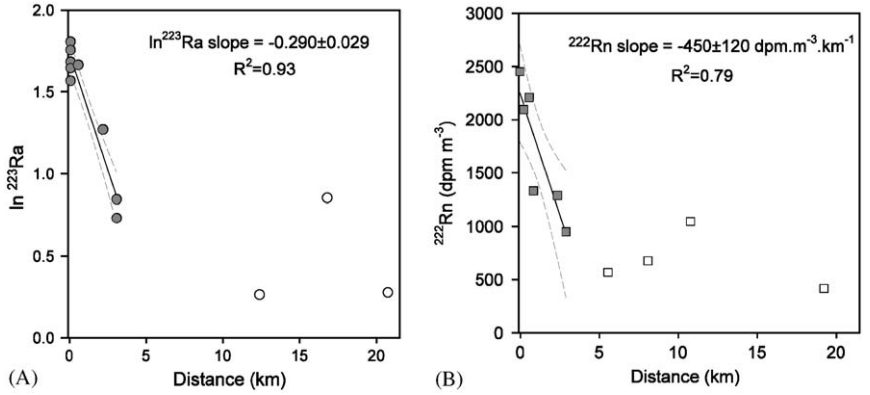

Fig. 4. (A) Natural logarithm of ^{223}Ra concentration over distance on transect from study site to Gardiners Bay that is used to calculate the mixing coefficient in West Neck Bay. (B) Radon-222 activities (dpm m^{-3}) along the same transect. Both plots have regression lines shown for the West Neck Bay part of transect (closed symbols). The open symbols represent values measured in Gardiners bay, which were not used in the regression. The dashed lines represent the 95% confidence intervals around the regression.

which we calculate a mixing coefficient of $8.6 \pm 1.2\,m^2\,s^{-1}$ based on Eq. (1):

$$\text{slope} = \sqrt{\frac{\lambda_{223}}{K_h}}. \quad (1)$$

This model assumes that all groundwater discharge and radium input occurs at the coastline around the head of the bay and we neglect any inputs that might occur along the length of the channel. Should such inputs occur that would mean that the applied ^{223}Ra slope is too small and thus the calculated mixing too fast. The flux of ^{226}Ra from the study site can then be calculated as the product of the concentration gradient of ^{226}Ra and the mixing coefficient derived from ^{223}Ra. For a linear ^{226}Ra concentration gradient of $-0.84 \pm 0.23\,dpm\,m^{-3}\,km^{-1}$ calculated from the 4-km long part of the transect and the assumption that the tracer is transported in a 2.6 m deep layer (average depth in WNB), the offshore ^{226}Ra flux is $(1.6 \pm 0.5) \times 10^6\,dpm\,km^{-1}\,d^{-1}$. Assuming that this flux is in steady state, ^{226}Ra must be balanced by an input in the coastal zone—most likely from SGD. Since there are no creeks or rivers emptying into the bay, we assume that groundwater discharge is the sole source of radium at our study site in WNB. From previous measurements (Paulsen et al., 2001) we know that SGD is high in this area and that compared to SGD, sediment resuspension and surface runoff are likely negligible sources of radium. According to the ultrasonic seepage meter measurement results at the field site, seepage meters positioned beyond ~45 m from the shore measured very low (up to 11 cm day^{-1}) groundwater flow compared to those located at 0–35 m (measured SGD rates up to 100 cm day^{-1}). Extending this decreasing trend offshore results in negligible discharge at 50 m. Therefore it appears that the groundwater discharge is most intensive in a 50-m wide section along the shoreline. Using the measured ^{226}Ra activities in seepage meters (average $= 220 \pm 130\,dpm\,m^{-3}$, $n = 18$, Table 1) we converted the radium flux to a water flux by dividing by this concentration. This results in a groundwater seepage flux of $7 \pm 5\,m^3\,m^{-1}\,d^{-1}$ i.e., $7\,m^3$ of groundwater flowing into the sea per unit meter of shoreline per day in the study area. Assuming a 50-m wide seepage face, this flow translates into an upward velocity flux of $0.15\,m\,d^{-1}$. We can get a conservative (lower limit) estimate of SGD using the maximum measured ^{226}Ra activity ($370 \pm 16\,dpm\,m^{-3}$ from a seepage meter), which produces an apparent seepage flow of $4 \pm 1\,m^3\,m^{-1}\,d^{-1}$ or an upward flux of $0.09\,m\,d^{-1}$.

4.2. Offshore flux of ^{222}Rn

The similar radioactive–conservative behavior and concurrent measurements of radon and radium isotopes allow us to use the horizontal mixing coefficient derived from ^{223}Ra to calculate the offshore flux of radon from our study site. Quantification of the loss of ^{222}Rn from nearshore waters via horizontal transport is an important component of the radon mass balance. Under the assumption that the water column is well mixed, the linear radon activity gradient along the study

transect (Fig. 4b) was $-450 \pm 120\,\mathrm{dpm\,m^{-3}\,km^{-1}}$. The negative trend is due to losses by mixing with water with low radon activity, radioactive decay, and atmospheric evasion. Both radioactive decay and atmospheric loss are most important for the more distant points along the transect because of increasing age (time since radon enters water from near-shore seepage). We calculate the radon flux offshore from the WNB study area by multiplying the linear portion of the ^{222}Rn gradient along the transect ($-450\,\mathrm{dpm\,m^{-3}\,km^{-1}}$) by the horizontal mixing coefficient derived from analysis of the ^{223}Ra gradient ($8.6\,\mathrm{m^2\,s^{-1}}$) and the average depth of WNB (2.6 m). This calculation results in a total ^{222}Rn offshore flux of $(3.6 \pm 1.0) \times 10^4\,\mathrm{dpm\,m^{-1}\,h^{-1}}$. In order to convert this seaward flux to a flux of ^{222}Rn from the nearshore seepage face on the seabed, we divide the offshore flux by the estimated width of the seepage face (50 m). The resulting ^{222}Rn flux is equal to $730 \pm 260\,\mathrm{dpm\,m^{-2}\,h^{-1}}$. This independent estimate of the loss of radon via mixing will assist us to constrain the mass balance of ^{222}Rn in our continuous radon model approach for assessing SGD (see Section 4.3).

4.3. Calculation of SGD from continuous radon model

The continuous radon monitor provided high-resolution data on radon concentration in the water column at one location over time (Fig. 3). We used this record to quantify rates of groundwater discharge by calculating radon fluxes using a mass-balance approach (Burnett and Dulaiova, 2003). Using the continuous water level information and ^{226}Ra concentrations from spot measurements in the water column, we calculated the unsupported ^{222}Rn inventories for each 2-h long measurement interval. The inventories were then converted into radon flux expressed as the change in radon inventory over time, in our case over a 2-h period. These fluxes were corrected for tidal changes by subtracting any offshore radon brought to the site by the incoming tides and correcting for radon losses due to outgoing tides (Burnett and Dulaiova, 2003). These corrections were on the order of 10% of the total radon flux. The tidal range during our 7-day study was on average about 0.6 m. Radon losses by atmospheric evasion were calculated for each measurement interval. The total radon gas flux across air–water interface depends on the molecular diffusion produced by the concentration gradient across this interface and turbulent transfer governed primarily by wind speed. We used the gas exchange equations presented by Macintyre et al. (1995) that calculate the gas transfer across the sea–air interface using the radon concentration gradient, temperature and wind speed measured by our weather station at the study site. The wind speed ranged from 0.1 to $4.4\,\mathrm{m\,s^{-1}}$ with an average of $2.3\,\mathrm{m\,s^{-1}}$ and the calculated radon evasion flux represented 1–2% loss in the total radon inventory in the water per hour. In this manner we were able to calculate the net radon fluxes (Fig. 5) that represent the observed fluxes of ^{222}Rn into the water column with all necessary corrections except losses via mixing with lower radon activity waters offshore. From the net radon fluxes it is apparent that most of the radon enters the water column during low tide. The flux is always highest at low tide and lowest at high tides. We assume that the apparent negative fluxes observed in the diagram are due to mixing processes between coastal and offshore waters with lower radon concentration. We estimated these mixing losses for different periods based on the maximum absolute values of the observed negative fluxes. We assume that the maximum negative net fluxes are conservative estimate of the mixing loss as greater losses could be masked by concurrently higher inputs. Based on this assumption, the mixing losses would range between 500 and $1150\,\mathrm{dpm\,m^{-2}\,h^{-1}}$ with an average of $670\,\mathrm{dpm\,m^{-2}\,h^{-1}}$ over the 7-day measurement period. The short-dashed line in Fig. 5 shows this approach.

This estimated mixing loss is in a very good agreement with the independent estimate of mixing losses based on the eddy diffusion coefficient derived from ^{223}Ra as described in Section 4.2. That flux equals $730 \pm 260\,\mathrm{dpm\,m^{-2}\,h^{-1}}$ (Fig. 5, solid line). The dynamic changes in mixing are not reflected in the radium derived estimate but it represents a radon flux integrated over at least several days before and during the measurements.

In the radon mass-balance approach for assessing SGD, the estimated mixing losses are added to the net fluxes resulting in total radon flux. Dividing the total radon fluxes by the ^{222}Rn activity of the advecting fluids results in estimated water fluxes. The presumed ^{222}Rn activity in seepage water was estimated by measuring the radon activity in piezometers, wells, and seepage meters as well as sediment equilibration experiments (Corbett et al., 1998) where one measures the total amount of radon that a sediment can produce into a unit

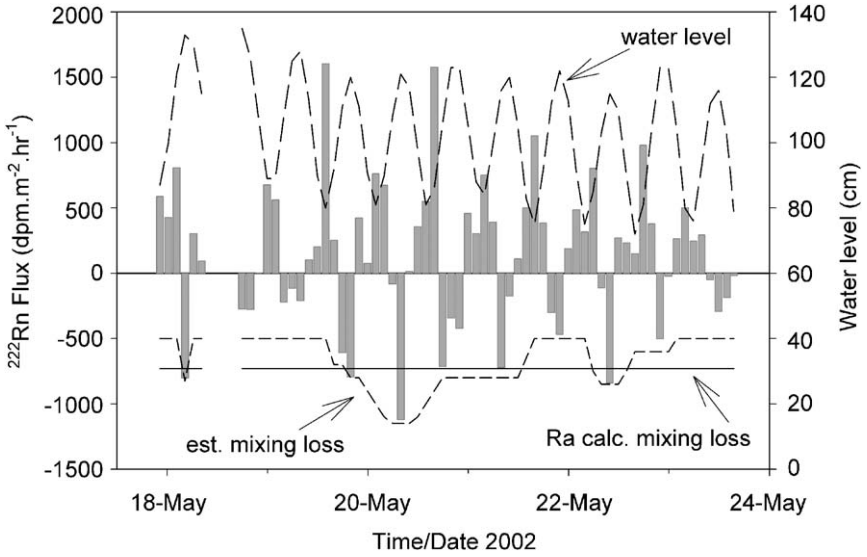

Fig. 5. Calculated net ^{222}Rn fluxes (bars) based on the change in inventories per unit time after corrections for tidal effects and atmospheric evasion. The mixing losses estimated via the maximum negative Rn fluxes (short-dashed line) and the ^{223}Ra-derived mixing loss (solid line), and water level (long-dashed line) are indicated on the figure.

amount of pore water. In general these different approaches resulted in very uniform radon activities with an average of 173 ± 17 dpm L^{-1} ($n = 10$). The well cluster S-1 was an exception with a much higher radon activity of 359 ± 10 dpm L^{-1}. We excluded the results from well S-1 from the average because we believe that these higher radon activities might be an effect of the anisotropy in the aquifer and based on the radon measurements in the benthic chambers they are not representative of the groundwater discharging into the bay.

We describe the SGD calculations using both mixing-loss scenarios. SGD calculated based on mixing losses estimated from the apparent negative net radon fluxes cycles between 0 and 34 cm d^{-1} with an average and standard deviation of 11 ± 7 cm d^{-1}. This flow is equivalent to 0–17 m^3 m^{-1} d^{-1} of groundwater flux per meter shoreline per day if we assume a seepage face of 50 m. Very similar results were estimated using radon fluxes calculated from the radium isotope-mixing approach, when the resulting SGD ranges between -5 and 32 cm d^{-1} with an average of 12 ± 7 cm d^{-1}. This flow is equivalent to -2–16 m^3 m^{-1} d^{-1}. The apparent negative advection rates are artifacts resulting from greater net radon losses than the average integrated value occurring over short periods. The calculated uncertainty of the individual SGD results is about 40%.

The SGD results assessed from the radon model using the radium-derived mixing are shown on Fig. 6 where the gray area represents the estimated uncertainty limits. The discharge clearly fluctuates with an apparent semidiurnal period of 12 h with a tidal range of about 0.6 m. The groundwater, and the radon that it carries, are responding to lower hydrostatic pressure at low tides, causing increased seepage and higher radon fluxes. A comparison between our measured net radon flux and the seepage rate at one point measured by a dye-dilution seepage meter (Sholkovitz et al., 2003) shows that all of the peaks in radon flux and groundwater discharge occur at low tides (Fig. 7). This supports the theory that with a presumably constant hydraulic head in the freshwater aquifer a decrease in hydrostatic pressure due to low tide results in increased seepage. The same dynamic seepage pattern was confirmed by several other automated seepage meters deployed at this site (Paulsen et al., 2001).

A similar model could not be set up for the methane fluxes because as Table 1 shows, there was no significant difference between the water column and groundwater methane concentrations. Overall, one must conclude that methane is not a good tracer of groundwater discharge in this glacial till setting. Methane is microbially formed in many eutrophic coastal marine sediments (i.e. Eckernforde bay; Schluter et al., 2004) but it seems that there was not sufficient organic matter within this aquifer

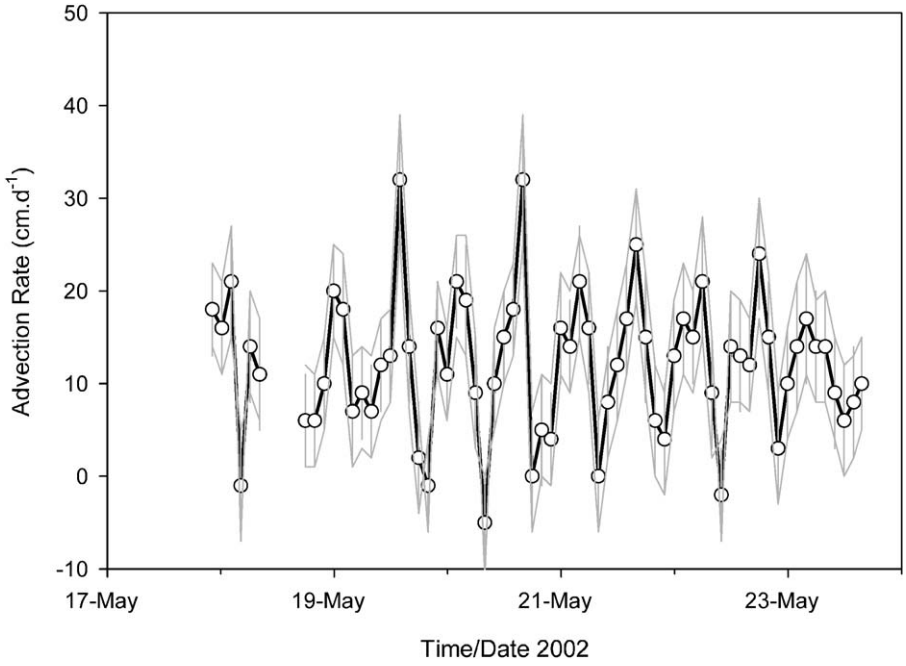

Fig. 6. Fluid advection rates assessed from the radon model using the Ra-derived mixing loss. The advection rates were calculated by division of the total radon flux by our best estimate of the radon concentration in the advecting fluids ($173{,}000 \pm 17{,}000\,\mathrm{dpm\,m^{-3}}$; see Table 2). The gray interval around the advection rate is the total combined uncertainty based on the errors of the analytical measurements as well as the estimated uncertainties of the atmospheric flux and mixing calculations.

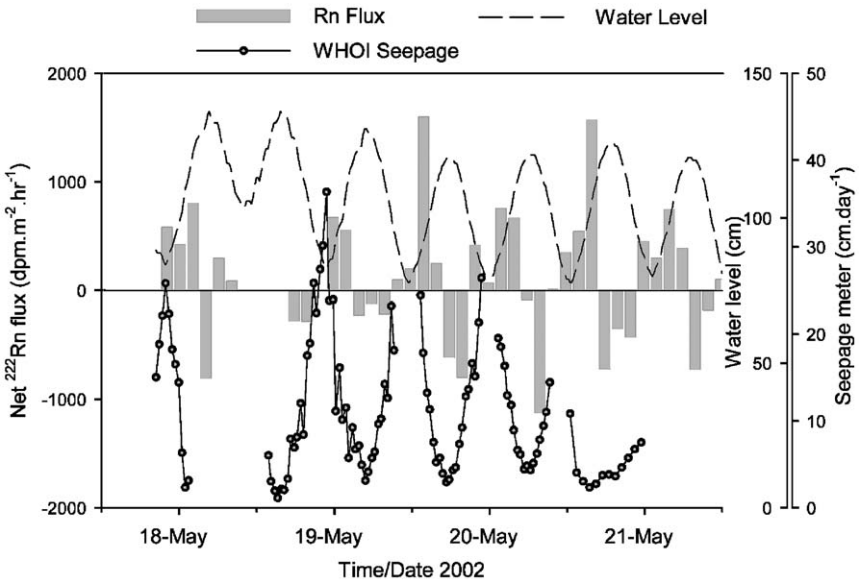

Fig. 7. Plot showing net ^{222}Rn fluxes, water level, and seepage rates measured by a dye-dilution seepage meter developed at Woods Hole Oceanographic Institution (Sholkovitz et al., 2003). Note that the maximum ^{222}Rn fluxes and the highest measured SGD tend to occur at low tides, while the main radon losses and lowest SGD occur at high tides.

matrix to produce a measurable SGD–methane signal. In other settings when CH_4 has been a successful tracer (Bugna et al., 1996; Cable et al., 1996b; Corbett et al., 1999; Kim and Hwang, 2002) there have been significantly greater CH_4 concentrations in groundwater relative to surface water

Table 3
Values of advection rates calculated by: (1) the continuous radon model using a mixing term estimated by inspection of "net fluxes"; (2) the radon model using a radium derived mixing term; and (3) calculated solely by the distribution of radium isotopes

Method	Specific discharge ($cm\,day^{-1}$)	Shoreline flux ($m^3\,m^{-1}\,day^{-1}$)
Radon: Inspection of Rn fluxes	Range: 0–34 Average: 11 ± 8	0–17 6 ± 4
Radon: ^{223}Ra mixing model	Range: 0–32 Average: 12 ± 7	0–16 6 ± 3
Ra Isotopes	15	7
WHOI meter—inshore WHOI meter—offshore	Range: 2–37 Range: 3–12	

For the radon balance approach the table shows the range in specific discharge that occurred between 17 May 2002 and 23 May 2002 and the average for the entire period. The same values are also expressed as a shoreline flux of groundwater per meter shoreline per day. Also shown are SGD values measured by the WHOI dye-dilution seepage meter positioned 10 m seaward of mean tide (inshore) and 20 m seaward of mean tide (offshore).

due to greater concentration of organic materials in the aquifer matrix.

4.4. SGD results determined using seepage meters

Groundwater discharge measurements were done using various types of seepage meters deployed at the site at the same time as the tracer study. The different meters included manual, dye-dilution, ultrasonic and continuous-heat type seepage meters. Estimates of the shoreline flux based on manual, dye-dilution (Fig. 7), and continuous-heat type seepage meters were $2–6\,m^3\,m^{-1}\,day^{-1}$. On the other hand, the ultrasonic seepage meter deployed at different locations from 0 to 50 m offshore measured a total integrated seepage of $18\,m^3\,m^{-1}\,day^{-1}$. This higher value may be attributed to the influence of a pier that ran perpendicular to the shoreline. The pilings of the pier had apparently pierced a shallow aquitard allowing local discharge of groundwater. The ultrasonic meter was deployed at locations near the pier and thus may have a high bias.

The resulting SGD rates from the different tracer approaches and the dye-dilution seepage meter are shown in Table 3. The advection rates shown include Rn estimates using the ^{223}Ra-mixing coefficient and mixing by inspection, the concentration gradient of ^{226}Ra, and the dye-dilution seepage meter. The table shows both the groundwater advection rate (specific discharge, $cm\,day^{-1}$) and flux per unit width of shoreline ($m^{-3}\,m^{-1}\,day^{-1}$).

5. Summary

The combination of radon and radium isotopes proved to be an excellent tool for revealing the magnitude and temporal variation of SGD in our study area in West Neck Bay. Methane could not be used to make SGD estimates in the glacial till environment of West Neck Bay because of its low concentration in groundwater. Radium isotopes provided information about material transport in the embayment. Using ^{223}Ra we calculated a horizontal eddy diffusivity coefficient of $8.6\,m^2\,s^{-1}$. We used this coefficient to make an independent estimate of the mixing loss of Rn for our continuous radon model. The resulting Rn flux by mixing was $730\,dpm\,m^{-2}\,h^{-1}$. This is in a good agreement with our conservative estimate ($500–1100\,dpm\,m^{-2}\,h^{-1}$) that is based on inspection of the net radon fluxes in the continuous radon mass-balance model.

All approaches produced results that were overlapping and in the range of seepage meter results. The continuous radon mass-balance approach using the mixing losses from inspection of Rn fluxes produced an estimate of $6\,m^3\,m^{-1}\,day^{-1}$ (average of $0–17\,m^3\,m^{-1}\,day^{-1}$) and gave very valuable information about the temporal variation of SGD. The calculated SGD flux from the radon model using the Ra-derived mixing was also $6\,m^3\,m^{-1}\,day^{-1}$ (average of $0–16\,m^3\,m^{-1}\,day^{-1}$) and the flux calculated using Ra isotopes alone was $4–7\,m^3\,m^{-1}\,day^{-1}$. These results are in agreement with the fluxes measured by various types of seepage meters deployed at the site. Estimates of the shoreline flux based on manual, dye-dilution, and continuous-heat

type seepage meters were 2–6 $m^3 m^{-1} day^{-1}$. On the other hand, the ultrasonic seepage meter deployed at different locations from 0 to 50 m offshore measured a total integrated seepage of 18 $m^3 m^{-1} day^{-1}$. We should also mention that the tracers, measured in the water column, integrate a larger area than the seepage meters. In addition, conductivity measurements showed that a significant portion of nearshore SGD measured by the seepage meters was fresh water while the radiotracers integrating a larger area than seepage meters reflected total flow comprised of both fresh and saline water.

Despite some uncertainty about the best-integrated seepage values at the site, the continuous measurement techniques (Rn-model and seepage meters) all agree that there is a reproducible pattern of higher SGD flux during low tides. Both the concentrations of radon and the net radon fluxes (Figs. 3, 5 and 7) showed that the highest radon input to the water column is at low tides. The same pattern was confirmed by automated seepage meters deployed in the same area (Paulsen et al., 2001; Sholkovitz et al., 2003).

Acknowledgments

We thank the organizers of the experiments and the teams from Stony Brook University, Cornell Cooperative Extension, and the Suffolk County Department of Health for the logistical and personnel support during the experiment. We thank C. E. Stringer and R. N. Peterson for their help with fieldwork and sample analysis. The SGD intercomparison experiment was partially funded by SCOR, LOICZ, and UNESCO (IOC and IHP). W. C. Burnett acknowledges support from CICEET (Grant# 1368-810-41) and ONR (Grant# 1368-769-27). J. P. Chanton acknowledges support from Seagrant (R\C-E-44). The WHOI researchers acknowledge funding from CICEET (#NA07OR0351, NA17OZ2507).

References

Boehm, A.B., Shellenbarger, G.G., Paytan, A., 2004. Groundwater discharge: Potential association with fecal indicator bacteria in the surf zone. Environmental Science and Technology 38 (13), 3558–3566.

Bokuniewicz, H., 2001. Toward a coastal ground-water typology. Journal of Sea Research 46, 99–108.

Bugna, G.C., Chanton, J.P., Cable, J.E., Burnett, W.C., Cable, P.H., 1996. The importance of groundwater discharge to the methane budgets of nearshore and continental shelf waters of the northeastern Gulf of Mexico. Geochimica et Cosmochimica Acta 60 (23), 4735–4746.

Burnett, W.C., Dulaiova, H., 2003. Estimating the dynamics of groundwater input into the coastal zone via continuous radon-222 measurements. Journal of Environmental Radioactivity 69, 21–35.

Burnett, W.C., Taniguchi, M., Oberdorfer, J., 2001a. Measurement and significance of the direct discharge of groundwater into the coastal zone. Journal of Sea Research 46, 109–116.

Burnett, W.C., Kim, G., Lane-Smith, D., 2001b. A continuous radon monitor for assessment of radon in coastal ocean waters. Journal of Radioanalytical and Nuclear Chemistry 249, 167–172.

Burnett, W.C., Chanton, J.P., Christoff, J., Kontar, E., Lambert, M., Moore, W.S., O'Rourke, D., Smith, C., Smith, L., Taniguchi, M., 2002. Assessing methodologies for measuring groundwater discharge to the ocean. EOS 83, 117–123.

Cable, J.E., Burnett, W.C., Chanton, J.P., Weatherly, G., 1996a. Modeling groundwater flow into the ocean based on ^{222}Rn. Earth and Planetary Science Letters 144, 591–604.

Cable, J.E., Bugna, G.C., Burnett, W.C., Chanton, J.P., 1996b. Application of ^{222}Rn and CH_4 for assessment of groundwater discharge to the coastal ocean. Limnology & Oceanography 41, 1347–1353.

Chanton, J.P., Burnett, W.C., Dulaiova, H., Corbett, D.R., Taniguchi, M., 2003. Seepage rate variability in Florida Bay driven by Atlantic tidal height. Biogeochemistry 66, 187–202.

Charette, M.A., Buesseler, K.O., Andrews, J.E., 2001. Utility of radium isotopes for evaluating the input and transport of groundwater-derived nitrogen to a Cape Cod estuary. Limnology & Oceanography 46 (2), 465–470.

Corbett, D.R., Burnett, W.C., Cable, P.H., Clark, S.B., 1998. A multiple approach to the determination of radon fluxes from sediments. Journal of Radioanalytical and Nuclear Chemistry 236, 247–252.

Corbett, D.R., Chanton, J.P., Burnett, W.C., Dillon, K., Rutcowski, C., Fourqurean, J., 1999. Patterns of groundwater discharge into Florida Bay. Limnology & Oceanography 44, 1045–1055.

Corbett, D.R., Dillon, K., Burnett, W.C., Chanton, J.P., 2000. Estimating the groundwater contribution into Florida Bay via natural tracers, ^{222}Rn and CH_4. Limnology & Oceanography 45, 1546–1557.

D'Elia, C.F., Webb, K.L., Porter, J.W., 1981. Nitrate-rich groundwater inputs to Discovery Bay, Jamaica: A significant source of N to local coral reefs? Bulletin of Marine Science 31, 903–910.

DiLorenzo, J.L., Ram, R.V., 1991. Flushing-time estimates for West Neck Harbor: a small tidal embayment of the Peconic Bays, New York. Report—Najarian Associates, L.P. Eatontown, NJ, 44p.

Johannes, R.E., 1980. The ecological significance of the submarine discharge of groundwater. Marine Ecology-Progress Series 3, 365–373.

Kelly, R.P., Moran, S.B., 2002. Seasonal changes in groundwater input to a well-mixed estuary estimated using radium isotopes and implications for coastal nutrient budgets. Limnology & Oceanography 47 (6), 1796–1807.

Kim, G., Hwang, D.-W., 2002. Tidal pumping of groundwater into the coastal ocean revealed from submarine ^{222}Rn and CH_4 monitoring. Geophysical Research Letters 29 (14), 23–27.

Kim, G., Ryu, J.W., Yang, H.S., Yun, S.T., 2005. Submarine groundwater discharge (SGD) into the Yellow Sea revealed by Ra-228 and Ra-226 isotopes: implications for global silicate fluxes. Earth and Planetary Science Letters 237 (1-2), 156–166.

Krest, J.M., Harvey, J.W., 2003. Using natural distributions of short-lived radium isotopes to quantify groundwater discharge and recharge. Limnology & Oceanography 48 (1), 290–298.

Laroche, J., Nuzzi, R., Waters, R., Wyman, K., Falkowski, P.G., Wallace, D.W.R., 1997. Brown tide blooms in Long Island's coastal waters linked to interannual variability in groundwater flow. Global Change Biology 3, 397–410.

Macintyre, S., Wanninkhof, R., Chanton, J.P., 1995. Trace gas exchange across the air-sea interface in freshwater and coastal marine environments. In: Matson, P.A., Harris, R.C. (Eds.), Biogenic Trace Gases: Measuring Emissions from Soil and Water. Blackwell Science Ltd, Oxford, pp. 52–97.

Michael, H.A., Mulligan, A.E., Harvey, C.F., 2005. Seasonal oscillations in water exchange between aquifers and the coastal ocean. Nature 436 (7054), 77–87.

Moore, W.S., 1976. Sampling ^{228}Ra in the deep ocean. Deep Sea Research and Oceanographic Abstracts 23, 647–651.

Moore, W.S., 1996. Large groundwater inputs to coastal waters revealed by ^{226}Ra enrichments. Nature 380, 612–614.

Moore, W.S., 1999. The subterranean estuary: a reaction zone of ground water and sea water. Marine Chemistry 65, 111–125.

Moore, W.S., 2000a. Determining coastal mixing rates using radium isotopes. Continental Shelf Research 20, 1993–2007.

Moore, W.S., 2000b. Ages of continental shelf waters determined from ^{223}Ra and ^{224}Ra. Journal of Geophysical Research 105 (9), 22,117–22,122.

Moore, W.S., Arnold, R., 1996. Measurement of ^{223}Ra and ^{224}Ra in coastal waters using delayed coincidence counter. Journal of Geophysical Research 101 (C1), 1321–1329.

Paulsen, J.R., Smith, C.F., O'Rourke, D., Wong, T.-F., 2001. Development and evaluation of an ultrasonic ground water seepage meter. Ground Water 39 (6), 904–911.

Sauter, E.J., Laier, T., Andersen, C.E., Dahlgaard, H., Schluter, M., 2001. Sampling of sub-seafloor aquifers by a temporary well for CFC age dating and natural tracer investigations. Journal of Sea Research 46, 177–185.

Schluter, M., Sauter, E.J., Andersen, C.E., Dahlgaard, H., Dando, P., 2004. Spatial distribution and budget for submarine groundwater discharge in Eckernförde Bay (W-Baltic Sea). Limnology and Oceanography 49 (1), 157–167.

Schubert, C.E., 1998. Areas contributing ground water to the Peconic estuary, and ground-water budgets for the North and South forks and Shelter Island, Eastern Suffolk County, New York. US Geological Survey, Water resources investigations report 97-4136.

Sholkovitz, E., Herbold, C., Charette, M., 2003. An automated dye-dilution based seepage meter for time-series measurement of submarine groundwater discharge. Limnology & Oceanography: Methods 1, 16–28.

Stringer, C.E., Burnett, W.C., 2004. Sample bottle design improvements for radon emanation analysis of natural waters. Health Physics 87, 642–646.

Taniguchi, M., Burnett, W.C., Cable, J.E., Turner, J.V., 2002. Investigation of submarine groundwater discharge. Hydrological Processes 16, 2115–2129.

Valiela, I., Costa, J., Foreman, K., Teal, J.M., Howes, B., Aubrey, D., 1990. Transport of groundwater-borne nutrients from watersheds and their effects on coastal waters. Biogeochemistry 10, 177–197.